Journal of Applied Physics

RESEARCH ARTICLE | MARCH 30 2022

Thermal transport in silver-coated polymer sphere composites by the bidirectional 3ω method

Susanne Sandell; Thorstein Wang; Emigdio Chávez-Ángel; ... et. al

Journal of Applied Physics 131, 125107 (2022)
https://doi.org/10.1063/5.0080682

AIP Publishing

Journal of Applied Physics METHOD scitation.org/journal/jap

Thermal transport in silver-coated polymer sphere composites by the bidirectional 3ω method

Cite as: J. Appl. Phys. **131**, 125107 (2022); doi: 10.1063/5.0080682
Submitted: 2 December 2021 · Accepted: 12 March 2022 ·
Published Online: 30 March 2022

Susanne Sandell,[1] Thorstein Wang,[1] Emigdio Chávez-Ángel,[2] Helge Kristiansen,[1,3] Zhiliang Zhang,[1] and Jianying He[1,a)]

AFFILIATIONS

[1]NTNU Nanomechanical Lab, Department of Structural Engineering, Norwegian University of Science and Technology (NTNU), 7491 Trondheim, Norway
[2]Catalan Institute of Nanoscience and Nanotechnology (ICN2), (ICN-CSIC) Barcelona, Campus UAB, E08193 Bellaterra, Spain
[3]Conpart AS, NO-2013 Skjetten, Norway

[a)]**Author to whom correspondence should be addressed:** jianying.he@ntnu.no

ABSTRACT

The bidirectional 3ω method is an electrothermal technique that is commonly used to obtain the thermal conductivity of materials such as liquids, biological samples, and pastes. In this work, an epoxy-based adhesive was filled with monodisperse 10 μm polymethyl methacrylate spheres coated with silver thin films (AgPS), such that a metallic network that dominated the thermal transport was formed through the composite. The bidirectional 3ω method was used to obtain the thermal conductivity of the conductive adhesive at different volume fractions of AgPS. For 50 vol.% AgPS, corresponding to 3.4 vol.% silver, the thermal conductivity was 2.03 ± 0.21 W m^{-1} K^{-1}. The results show that the thermal conductivity is strongly correlated with the AgPS volume fraction, while maintaining a volume fraction of silver far below the commercial silver paste, which has typical filler fractions of 40 vol.% silver. The results of this work were compared to thermal measurements of the same material by other techniques, and advantages and disadvantages of the methods were finally discussed.

I. INTRODUCTION

Thermal management is critical to the lifetime, performance, and reliability of electronic devices.[1–4] In order to avoid overheating, it is desirable to increase the heat dissipation, both at the "local" single transistor level as well as at the "global" electronic packaging levels.[5] Polymers are widely used in electronic packaging as the matrix material in composites, such as thermal interface materials[6] and conductive adhesives.[7] The bulk thermal conductivity of most polymers is very low, on the order of 0.1–0.5 W m^{-1} K^{-1}, which limits their heat dissipation capabilities.[8] To increase the thermal and/or electrical conductivity of conductive adhesives, conductive fillers are often added to the polymer matrix. These fillers can be carbon-based, metallic, ceramic or, more recently, boron nitride-based.[7] The electrically conductive filler particles form a percolating network through the polymer adhesive matrix, significantly increasing the electrical and thermal conductivity.[9] In order to form the percolating network, a filler fraction of between 25 and 40 vol.% is usually required. When the filler fraction is high enough to form an electrically conductive percolating network in all directions through the matrix, the composite is called an isotropic conductive adhesive (ICA). ICAs are an environmentally friendly alternative to soldering as they are lead-free, and they are typically used for material systems that require lower processing temperatures. They can also be applied to materials that are difficult to wet with traditional solders, such as glass and ceramics. Conventional ICAs are composed of an adhesive matrix with embedded metal flakes or particles for both electrical and thermal conductivity. Due to their excellent electrical and thermal properties, silver particles are often used. Although increased electrical conductivity (σ) is often the goal when optimizing ICA processes, this article will focus solely on increasing thermal conductivity (κ). Conventional ICAs require a high silver content, up to 40 vol.%, to achieve thermal conductivities at around $\kappa \approx 3$ W m^{-1} K^{-1} using the laser flash (LF) technique.[10]

In order to reduce the silver content, monodisperse micron-sized polymer spheres coated with thin silver films (AgPS)

embedded in epoxy have proven themselves as a viable alternative to the conventional ICAs.[11–20] This material system, hereafter referred to as AgPS-ICA, has a large advantage over the conventional ICAs due to the significant reduction in costly silver.

AgPS-ICAs have yielded thermal conductivities similar to the conventional ICAs at Ag filler fractions of around 3 vol.% measured using both steady state (SS) and LF techniques.[21,22] For both methods, a clear correlation was observed between AgPS volume fraction and thermal conductivity. However, for larger AgPS volume fractions (>40 vol.%), values measured by the SS method are consistently around 35% higher than those measured by the transient LF method. This discrepancy is possibly due to the volumetric constraint exerted on the sample during curing and measurement by the SS method. However, the thermal transport mechanisms of this novel AgPS-ICA need further investigation,[22] and the best suited thermal characterization technique is yet to be found.

In this work, we measured the thermal conductivity of AgPS-ICAs using a self-built electrothermal characterization technique, commonly referred to as the 3ω method. To the best of our knowledge, this is the first attempt at thermal characterization of this novel ICA by 3ω. The results obtained here are discussed in the context of the previous measurements by SS and LF, and finally these techniques are compared in terms of advantages and disadvantages.

II. 3ω METHOD

The 3ω method is a thermal characterization technique widely used for the determination of thermal conductivity. It was developed in the 1990s by Cahill[23,24] and is a transient electrothermal technique which induces a temperature fluctuation by applying a transient (AC) current to a thin microfabricated metal line, $I_{app}(t) = I_0\cos(\omega t)$. The metal line acts as both heater and sensor. Hereafter, for convenience, the metal line will be referred to as the *heater*. Due to the applied AC current, the heater temperature oscillates at an angular frequency of 2ω. The temperature fluctuation in the heater, in turn, induces a fluctuation in the electrical resistance, R_e, which is detected by measuring the voltage, V, across the heater. This signal relates to the temperature fluctuation, $\Delta T_{2\omega}$. $\Delta T_{2\omega}$ can then be used to determine the thermal properties of the substrate. The measured temperature oscillation is given by[23,24]

$$\Delta T_{2\omega} = \frac{2}{\beta}\frac{V_{3\omega,RMS}}{V_{0,RMS}} \tag{1}$$

where V_0 and $V_{3\omega}$ are total and third harmonic voltages, respectively, across the heater. As a rule of thumb, $V_{3\omega}$ is typically three orders of magnitude larger than V_0.[25] β is the temperature coefficient of electrical resistivity,

$$\beta = \frac{1}{R_{e,0}}\frac{dR_e(T)}{dT}, \tag{2}$$

where $R_{e,0}$ is the electrical resistance at a reference temperature T_0. The thermal conductivity κ of the substrate is then given by[23,24]

$$\Delta T_{2\omega} = \frac{1}{2b}\int_{-b}^{b}\Delta T_{2\omega}(x)dx = \frac{P_l}{\pi\kappa}\int_0^\infty \frac{\sin^2(kb)}{(kb)^2\sqrt{k^2+q^2}}dk, \tag{3}$$

where b is the half-width of the heater, κ is the substrate's thermal conductivity, and P_l is the AC power per unit length of the heater. The integration variable, k, is the wavenumber. $q = \sqrt{\frac{i2\omega}{\alpha}}$, and α is the thermal diffusivity. The quantity $l_{th} = |\frac{1}{q}|$ is the thermal penetration depth, which is the depth at which the thermal wave propagates into the substrate during one cycle of AC heating. κ is found by least squares fitting of the measured temperature drop in Eqs. (1)–(3).

The conventional 3ω method requires microfabrication of the heater on top of the sample to be measured, which requires the sample to be solid, dry, and flat. While useful for thin films and rigid substrates, it is impractical for a wide range of samples. The bidirectional 3ω method was developed[26–29] in order to measure thermal conductivity for samples such as nanofluids,[30] biological tissues,[31] and thermal pastes.[32] It allows for the sample to be deposited onto a platform where the heater is already deposited [Fig. 2(a)]. It has the additional advantage of requiring only a small droplet of the sample material in order to accurately measure the thermal conductivity.

The bidirectional 3ω method extends the conventional methodology by considering heat transfer through two semi-infinite media above and below the heater line, as indicated schematically in Fig. 2(b). The main principles are given here, and the reader is referred to the work by Oh *et al.*[28] and the supplementary information in Rodríguez-Laguna *et al.*[30] for a more detailed description. The sample of interest is placed on a quartz substrate with a passivated heater line, the *reference*, as shown in Figs. 2(a) and 2(b). The relation between the temperature oscillations is as follows:[28]

$$\frac{1}{\Delta T_{\text{eff}}} = \frac{1}{\Delta T_{\text{ref}}} + \frac{1}{\Delta T_{\text{sam}}}, \tag{4}$$

where ΔT_{eff} is the measured temperature oscillation of the heater. ΔT_{ref} is the temperature oscillation of the heater in a system consisting of only the reference substrate. The temperature spread in the thin dielectric layer is also included in ΔT_{ref}. ΔT_{sam} is the temperature oscillation in the heater in a system consisting only of the sample. The thermal resistance at the sample/reference interface is neglected. First, a calibration measurement of the reference is performed to determine ΔT_{ref}. Then, the sample is applied, and a new thermal measurement is done. The sample's temperature rise is then given by rewriting Eq. (4),

$$\Delta T_{\text{sam}} = \left(\frac{1}{\Delta T_{\text{eff}}} - \frac{1}{\Delta T_{\text{ref}}}\right)^{-1}. \tag{5}$$

Here, ΔT_{sam} is then taken as $\Delta T_{2\omega}$ in Eq. (1) from which the thermal conductivity of the sample, κ, is found by least squares fitting to Eq. (3).

V_0 measured between the inner voltage pads of the metal strip is a sum of the 1ω and 3ω components, with the latter being three

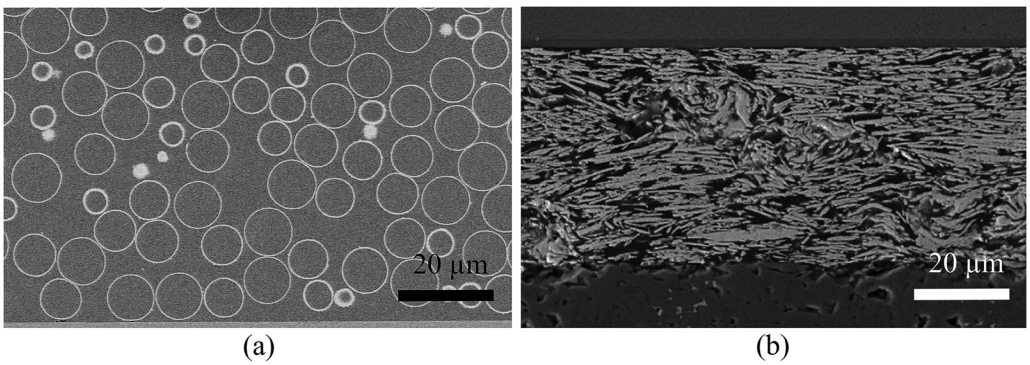

FIG. 1. (a) SEM image of the cross section of an ICA containing 35 vol.% AgPS (2.2 vol.% silver), and (b) SEM image of a commercial ICA with 31 vol.% silver flakes. (b) was adapted from Ref. 11.

orders of magnitude smaller than the first. A conditioning circuit (Fig. 3) is able to cancel out the $V_{1\omega}$ signal, leaving only the $V_{3\omega}$ signal to be detected by the lock-in amplifier.

The current source, a Keithley 6221 (OH, USA), outputs a high-purity sinusoidal current $I_{app}(t)$ of frequency ω that is applied across the metal line. In order to make sure that the heating power is always constant at 2 mW, the magnitude of $I_{app}(t)$ is adjusted iteratively by measuring the voltage across a 10 Ω resistor element, and calculating the current $I_0 = V_{I_0}/(10\,\Omega)$, as indicated in Fig. 3. Also shown in the figure is V_0, which is measured between the voltage pads. I_0 and V_0, along with the temperature T of a PT100 element placed in close proximity to the sample, are measured using a data aquisition box (DAQ) of type NI cDAQ-9174. The voltages associated with I_0 and V_0 are measured using BNC connections to a NI9215 module, whereas T is measured in a 4-wire configuration to a NI9217 module. The data acquisition modules are all from National Instruments (Austin, TX, USA).

To remove the fundamental (1ω) component, the voltage amplitude measured across the variable resistance R_D is adjusted iteratively. This is done by varying the resistance R_D until the amplitude of the measured voltage V_ω matches the amplitude of the voltage measured across the heater line, $V_{\omega+3\omega}$. The resistance is varied using a M642 programmable resistance decade (Meatest, Brno, Czech Republic). When the voltages are matched, the final operational amplifier subtracts V_ω from $V_{\omega+3\omega}$, outputting $V_{3\omega}$, which is then measured using a DSP7265 lock-in amplifier (Signal Recovery, Oak Ridge, TN, USA). The operational amplifiers are polarized using a BP3002 DC power supply (Digimess, Leicester, UK). The measured signal is averaged by 10 measurements at each frequency.

The choice of heating frequency is an important source of uncertainty, since it determines the thermal penetration depth (or thermal wavelength) in the sample. If the frequency is too high, the measured signal will be dominated by the interface between the heater and sample. If too small, the signal will be dominated by the substrate or the interface between the substrate and platform. Other important sources of uncertainty in the measurement are the heater dimensions (film thickness, width, and length). For a more thorough discussion on measurement design rules for reducing uncertainty sources, see work by Dames.[33]

In these measurements, the heating frequency is chosen to ensure that the thermal penetration depth ($l_{th} = \sqrt{\alpha/2\omega}$) is several times smaller than the substrate and sample thickness. In this case, it was calculated that the sample was 3.4 times thicker than the penetration depth. This is to ensure that the oscillating temperature is localized well within the media of interest, and is insensitive to the boundary condition between them and the surroundings. However, we want to have a frequency low enough so that the thermal wave penetrates well into the sample and substrate, to not be affected by the thermal resistances associated with the interfaces near the heater. Also, the substrate and sample should "see" the heater as a 1D source, that is $b \to 0$. This is ensured by choosing frequencies such that $l_{th}/b > 5$, which is a design criteria for 1% error for this assumption.[33,34]

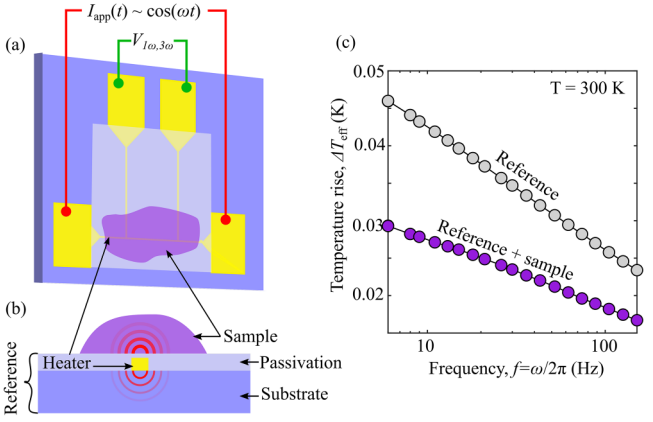

FIG. 2. (a) The reference chip for 3ω measurements, showing the applied current $I_{app}(t)$ and the measured voltage $V_{1\omega,3\omega}$ between the pads. The sample placement is shown in purple. (b) The reference chip with sample in the cross-sectional view. The bidirectional heat flow is illustrated schematically. (c) Measured temperature rise ΔT_{eff} of the reference chip and reference + sample, respectively.

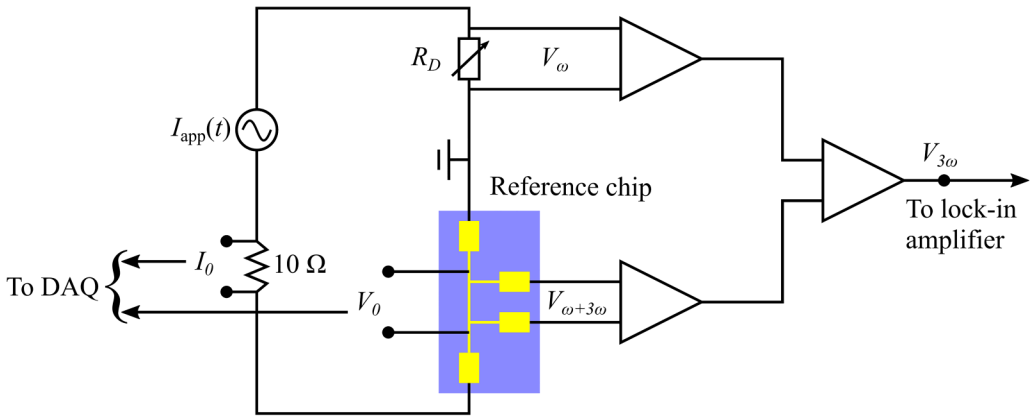

FIG. 3. The conditioning circuit of the 3ω setup.

III. SAMPLE FABRICATION

The reference chip was made by dicing a 0.5 cm thick fused quartz glass slide (SPI Supplies, PA, USA) into 1 cm^2 chips and microfabricating a 3ω structure on the chip. The 3ω structure was deposited through a hard mask by electron beam evaporation (AJA International, Inc., Scituate, MA, USA) of a Ti(2 nm)/Au(100 nm) layer. The hard mask is a 0.5 mm thick Ti plate with cut-outs corresponding to the 3ω structure, custom ordered from Veco (Veco B.V, Eerbeeck, The Netherlands). Since the sample in this case is electrically conductive, a dielectric layer of 50 nm Al_2O_3 was deposited by sputtering on top of the thin metal lines connecting the voltage pads.

The typical heater width is 20 μm, and its length (measured between the inner voltage pads) is 1 mm. The substrate material, fused quartz, has a thermal conductivity of 1.4 $W\,m^{-1}\,K^{-1}$ and a thermal diffusivity of 0.95 $mm^2\,s^{-1}$, according to the supplier's technical datasheet.[35]

The AgPS were prepared by a two-step swelling process, producing crosslinked PMMA particles with Diameters of 10 μm.[36] The 145 nm Ag shell was deposited by an electroless plating process. The adhesive matrix was prepared by mixing Araldite PY-302 epoxy resin with Jeffamine D-230 curing agent (both from Huntsman, Lindberg & Lund AS, Norway) in a 3:1 ratio by weight. AgPS was added to the matrix at 35, 40, 45, and 50 vol.%, respectively (see Fig. 1 and Table I). A small droplet (approximately 2.5 μl) of sample was applied to the 3ω reference chip in the sensor area as indicated by Figs. 2(a) and 2(b). Then, the sample-chip system was cured in a vacuum oven (Binder, Tuttlingen, Germany) at 150 ∘C for 40 min. The electrical connections to the voltage pads were made by manually wire bonding Au wires (diameter of 20 μm) between the pads and a chip holder with connections to BNC-cable inputs.

TABLE I. Volume and weight fractions of AgPS, calculated pre-cure density of AgPS-ICA and Ag volume and weight fraction of the four samples. The calculations are based on measured weight fractions and nominal densities given by the manufacturers of the constituents, and the nominal diameter and Ag film thickness of the AgPS.

Sample	AgPS (vol.%)	AgPS (wt.%)	Density AgPS-ICA (g/cm^3)	Ag (vol.%)	Ag (wt.%)
35AgPS	35	47.7	1.40	2.2	16.3
40AgPS	40	53.1	1.44	2.6	18.6
45AgPS	45	58.1	1.48	3.0	29.9
50AgPS	50	62.5	1.52	3.4	33.3

IV. RESULTS AND DISCUSSION

The thermal conductivities of the AgPS-ICA are plotted in Fig. 4 and shown in Table II. The reported error margins represent the standard error of the four individual measurements performed for each sample. A progressive, near-linear enhancement of thermal conductivity is seen as a function of AgPS volume fraction. For the largest AgPS volume fraction, 50 vol.%, a thermal conductivity of 2.03 $\pm$ 0.21 $W\,m^{-1}\,K^{-1}$ is reported from the 3ω measurement. From Table I, this corresponds to 3.4 vol.% silver. According to Kim *et al.*, a conventional silver flake ICA would need almost 20 vol.% silver to achieve a similar thermal conductivity.[37] Also shown in Fig. 4 are thermal conductivity measurements of the same AgPS-ICA from Kristiansen *et al.*[21] by the SS method and the LF method. In the SS method, the sample is cured at different thicknesses between two Cu rods and measured the thermal conductivity as $\kappa = Q/\nabla T$, where Q is the heat flow through the sample and ∇T is the temperature gradient across the sample. The LF is a transient method used to measure the thermal diffusivity α of the sample, the density ρ is measured by the immersion method, and the specific heat C_p is measured using differential scanning calorimetry (DSC). Then, the thermal conductivity is given by $\kappa = \alpha\rho C_p$.

From Fig. 4, it is evident that the two transient methods (3ω and LF) are in good agreement, following a similar trendline. However, the 3ω measurements yield thermal conductivities on

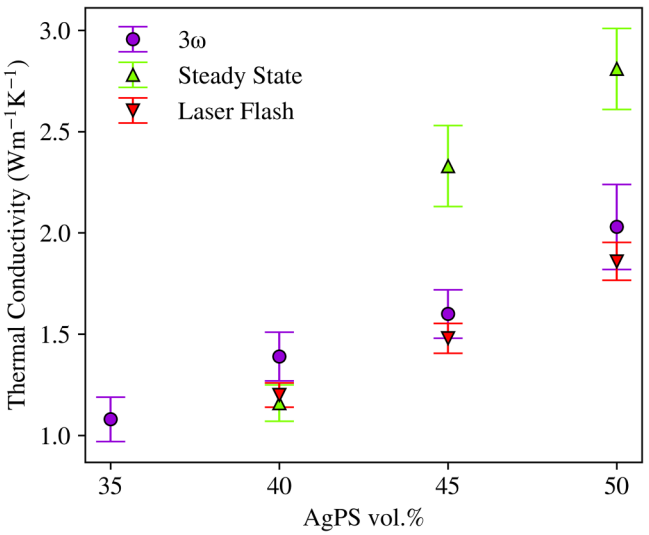

FIG. 4. Thermal conductivity of AgPS-ICAs for varying volume fractions of AgPS measured by 3ω, SS,[21] and LF[22] methods. The 3ω and LF measurements were done at room temperature, whereas the SS measurements were done at 40 °C. The error bars represent the standard error of the four data points for each sample.

average 11% above the LF measurements. The SS measurements give a thermal conductivity 16% below the 3ω measurements for the 40AgPS. For the 45 and 50AgPS sample, the SS measurements give thermal conductivities that are 46% and 38% above the 3ω measurements, respectively. Pettersen *et al.*[22] did LF measurements of AgPS-ICAs and showed that the technique for measuring the specific heat had a significant effect on the measured thermal conductivity for this sample system. However, this effect alone cannot explain the large discrepancies observed between the transient and steady state methods. Kristiansen *et al.*[21] pointed out that the large discrepancy in the values reported by the SS method occur for 45 and 50AgPS, which is above the percolation threshold. The increased thermal conductivity measured by the SS method could be due to the fixed bond line thickness (BLT) between the reference bodies during curing of the AgPS-ICA sample, which exerts a contact pressure on the sample due to thermal expansion. This could result in closer contact between the Ag shells, which conduct a large portion of the heat above the percolation threshold. This is in contrast to the curing method for the transient methods, in which the AgPS-ICA samples are allowed unconstrained thermal expansion. It can be argued that the SS method measures the thermal conductivity of AgPS-ICAs for a more realistic curing condition, as ICAs usually are cured between two bodies at a fixed BLT. In order to measure thermal properties under more realistic operating conditions, the 3ω sample curing process could be modified such that the sample is cured at a given BLT.

TABLE II. Thermal conductivity results for AgPS-ICAs from 3ω, SS, and LF methods.

vol.% AgPS	0	35	40	45	50
vol.% Ag	0	2.2	2.6	3.0	3.4
			Thermal conductivity (W m^{-1} K^{-1})		
3ω	…	1.08 ± 0.11	1.39 ± 0.12	1.60 ± 0.12	2.03 ± 0.21
SS	0.2	…	1.16 ± 0.09	2.33 ± 0.20	2.81 ± 0.20
LF	…	…	1.20 ± 0.060	1.48 ± 0.074	1.86 ± 0.093

TABLE III. Using the Wiedemann–Franz law, the electronic contribution to the thermal conductivity κ_e is calculated. The ratio κ_e/κ is calculated from the thermal conductivity measurements by the 3ω method.

Sample	σ (S/m)	κ_e (W m^{-1} K^{-1})	κ_e/κ
40AgPS	4.54×10^4	0.33	0.24
45AgPS	1.54×10^5	1.12	0.70
50AgPS	2.00×10^5	1.46	0.72

The results support the thermally conductive path theory, in which the filler particles at these high fill fractions are in contact with each other, as shown in Fig. 1(a). Thus, they form a thermally conductive network through the polymeric matrix material. We can calculate the electronic contribution to the total thermal conductivity using the Wiedemann–Franz law.[38] It states that the ratio of electronic contribution to thermal conductivity κ_e and electrical conductivity σ of a metal is proportional to temperature T,

$$\frac{\kappa_e}{\sigma} = L_0 T, \tag{6}$$

where the proportionality constant L_0 is called the Lorentz number and has the value of $L_0 = 2.44\times10^{-8}$ W Ω K^{-2}. From electrical conductivity measurements of the AgPS-ICA,[39] κ_e is calculated in Table III. It is worth mentioning here, that the increase in thermal conductivity resulting from a higher concentration of AgPS-ICA also increases the electrical conductivity of the samples.[40]

From Table III, we see that the κ_e/κ ratio is 0.24 for the 40AgPS sample, and 0.70 and 0.72 for the 45AgPS and 50AgPS sample, respectively. Although the silver thin films conduct a significant portion of the heat compared to their low volume fraction, the phonon contribution from the PMMA cores and the epoxy matrix still comprises a substantial part of the total effective thermal conductivity of the AgPS-ICA, especially for the 40AgPS sample. The thermal transport by electrons is limited to occur within the silver thin films or by tunneling across ultrathin epoxy layers between two AgPS. The thermal transport of the AgPS-ICA system has been discussed previously in the context of LF measurements,[22] which concluded that the thermal transport in the AgPS is dominated by the electronic heat transfer in the Ag layer. We believe a minor thermal transport mechanism deserves mention, which is the possibility of electron–phonon interactions across the Ag–polymer interfaces. When the heat is transported between the silver thin films and the nonconductive cores and matrix, this process is indeed believed to be dominated by phononic

TABLE IV. Comparison of thermal measurement techniques. Accuracy of 3ω based on the standard error of the measurements performed in this work.

Technique	Heating	Measurement time	Accuracy	Advantages	Disadvantages
3ω	Transient current	10 min	≈10%	Small sample size (μl)	Unrealistic curing conditions
				κ measured directly	Time consuming sample preparation and calibration
				Heating principle similar to operating conditions	
				<1 ∘C temperature gradient	
SS	Steady state	2 h	≈2%[1]	Standardized method (ASTM D5470)[44]	Time-consuming to reach steady state
				Simple experimental setup and data reduction	Radiation loss and thermal contact resistance
				κ measured directly	Requires specific size and shape of sample
				Sample is cured at a given BLT	Typically large (>20 °C) temperature gradient
LF	Transient laser	<1 min	3–5%[1]	Standardized method (ASTM E1461-13)[45]	Measures κ indirectly by measuring α
				<1 ∘C temperature gradient	Graphite coating, absolute planarity and accurate sample thickness measurements required
				Non-contact method	

interactions. The process of heat transfer across metal–dielectric interfaces have been widely studied by pulsed femtosecond laser heating, such as the study by Lyeo and Cahill.[41] They concluded that electrons contribute negligibly to heat transfer across a metal–dielectric interface. This gives us some insight into the heat transfer process between the silver thin films and the surrounding polymeric material. First, the hot electrons in the silver film thermalize by electron–phonon scattering within the metal film, a process which occurs on the picosecond timescale.[42] Then, the thermal energy of the metal's phonons is distributed to the polymer material through phonon–phonon scattering processes. The electron-phonon thermalization process is so rapid that it will not affect the 3ω measurements. This is because the heating events induced by the AC current are on the millisecond timescale, which is set by the frequency of the current (< 150 Hz). In conclusion, the measurement's timescale is much larger than the timescale associated with Electron–phonon thermalization events, which occur within picoseconds.

There is still no uniform testing standard for thermal conductivity measurements of polymer composites. Therefore, the obtained experimental values from different instruments are difficult to compare.[43] However, some advantages and disadvantages of the testing methods discussed here have been gathered in Table IV.

A main difference between the transient and steady state methods is the measurement time. In a steady-state measurement, the system as a whole must reach thermal equilibrium before measurements are done, which may take two hours. Furthermore, parasitic heat loss and thermal conduction through the thermocouples must be accounted for in steady state measurement, which is a major drawback for this technique. A significant advantage of 3ω over the SS method is that the error due to radiation loss is greatly reduced, due to the fact that thermal radiation scales with the characteristic size of the heater geometry. Even at 1000 K, the calculated error due to radiation is 2%,[46] which means that in our case with $\Delta T < 1$ K, this error source can be neglected. A drawback of the 3ω method is that the calibration of the β parameter is very time consuming, usually taking 3–4 h. This drawback can be overcome, however, either by (1) making the 3ω sensor reusable, or (2) standardizing the fabrication process of the 3ω sensor chips by using photolithography. It is then expected that two sensors from the same batch process should have the same β value. The option of making the sensor reusable could be realized by applying a thin nonstick layer on top of the sensor, such that the sample can be easily removed after measurement.

Contact thermal resistance is a major source of error in contact techniques. In 3ω, this is omitted by the choice of frequency band, avoiding the higher frequencies where the interface resistance contributes to the result. In the SS method, measurements of different sample thicknesses will eliminate the interface resistance, however, at the expense of longer time needed for testing. In this comparison, LF is the only non-contact method, since it uses a laser pulse to heat the front side of the sample and an IR detector to read the time-dependent temperature on the sample's backside. Radiation losses are accounted for by the thermal model used to fit the results. However, the sample preparation is not straightforward. The sample needs to be a specific size and shape, and is usually prepared by spraying a layer of graphite to act as an absorber. Accurate measurements of sample thickness are critical, as well as absolute planarity. The thickness of the sample is limited by the timescales associated with the heating and IR sensing. Commercial instruments can measure samples down to around 100 μ m depending on the thermal diffusivity of the material, and for thinner films, the 3ω method or thermoreflectance methods are needed.[47] A clear drawback of the LF technique, is

that it is an indirect way of measuring κ, by measuring the thermal diffusivity α and calculating the thermal conductivity by $\kappa = \rho\alpha C_p$, where the density ρ and specific heat C_p must be measured from separate experiments. So even if the LF measurement itself can be performed within seconds for most solids, the required additional measurements adds up to significantly more. Additionally, the separate measurements of ρ and C_p may result in larger errors.[22] Depending on the accuracy needed, reference measurements of samples with similar C_p and ρ can be used, omitting the measurements of these for the specific sample.

A drawback of the 3ω method when measuring conductive samples, as in this work, the need for a dielectric layer introduces an extra thermal resistance and reduces measurement accuracy. However, with a thin (50 nm) dielectric layer, the accuracy is negligibly affected in the low-frequency limit. This is due to the large thermal penetration depth (l_{th}) at the measurement frequencies compared to the dielectric layer thickness (t), with the first being over three orders of magnitude larger than the latter. Lubner *et al.*[31] showed that the dielectric layer had a negligible effect on the overall experimental error.

V. CONCLUSION

We report on the thermal transport in a novel AgPS-ICA that can achieve similar thermal and electrical conductivities as conventional ICAs with only a small fraction of the silver content. We measured the thermal conductivity of AgPS-ICAs using the bidirectional 3ω method. A progressive, near-linear enhancement of thermal conductivity was seen as a function of AgPS volume fraction. For 50 vol.% AgPS, corresponding to 3.4 vol.% silver, the thermal conductivity of the AgPS-ICA was $2.03 \pm 0.21\ \mathrm{W\,m^{-1}\,K^{-1}}$. For conventional silver flake ICAs, the volume fraction of silver would be nearly 20 vol.% silver in order to achieve a similar thermal conductivity. The results were discussed and compared to measurements by SS and LF, and the methods were compared in terms of applicability to AgPS-ICAs.

ACKNOWLEDGMENTS

The NTNU authors wish to acknowledge the Research Council of Norway for the support to this project through the FRINATEK Project No. 251068 with the title "Engineering Metal-Polymer Interface for Enhanced Heat Transfer (HEFACE)" and also for supporting the NTNU NanoLab through the Norwegian Micro- and Nano-Fabrication Facility, NorFab, Project No. 245963. ICN2 is supported by the Severo Ochoa program from the Spanish Research Agency (AEI, Grant No. SEV-2017-0706) and by the CERCA Programme/Generalitat de Catalunya. E.C.- Á acknowledges the support from the Spanish MICINN project SIP (No. PGC2018-101743-B-I00) and from EU Project NANOPOLY (No. GA 289061).

AUTHOR DECLARATIONS

Conflict of Interest

The authors have no conflicts to disclose.

DATA AVAILABILITY

Data sharing is not applicable to this article as no new data were created or analyzed in this study.

REFERENCES

[1]H. Chen, V. V. Ginzburg, J. Yang, Y. Yang, W. Liu, Y. Huang, L. Du, and B. Chen, "Thermal conductivity of polymer-based composites: Fundamentals and applications," Prog. Polym. Sci. Top. Vol. Hybrids **59**, 41–85 (2016).
[2]Y. Cui, M. Li, and Y. Hu, "Emerging interface materials for electronics thermal management: Experiments, modeling, and new opportunities," J. Mater. Chem. C **8**, 10568–10586 (2020).
[3]H. P. de Bock, D. Huitink, P. Shamberger, J. S. Lundh, S. Choi, N. Niedbalski, and L. Boteler, "A system to package perspective on transient thermal management of electronics," J. Electron. Packag. **142**, 041111 (2020).
[4]J. C. Kim, Z. Ren, A. Yuksel, E. M. Dede, P. R. Bandaru, D. Oh, and J. Lee, "Recent advances in thermal metamaterials and their future applications for electronics packaging," J. Electron. Packag. **143**, 010801 (2021).
[5]A. L. Moore and L. Shi, "Emerging challenges and materials for thermal management of electronics," Mater. Today **17**, 163–174 (2014).
[6]H. Ma, B. Gao, M. Wang, Z. Yuan, J. Shen, J. Zhao, and Y. Feng, "Strategies for enhancing thermal conductivity of polymer-based thermal interface materials: A review," J. Mater. Sci. **56**, 1064–1086 (2021).
[7]R. Aradhana, S. Mohanty, and S. K. Nayak, "A review on epoxy-based electrically conductive adhesives," Int. J. Adhes. Adhes. **99**, 102596 (2020).
[8]H. G. Chae and S. Kumar, "Making strong fibers," Science **319**, 908–909 (2008).
[9]*Advanced Flip Chip Packaging*, edited by H.-M. Tong, Y.-S. Lai, and C. Wong (Springer US, Boston, MA, 2013).
[10]M. Inoue, H. Muta, T. Maekawa, S. Yamanaka, and K. Suganuma, "Physical factors determining thermal conductivities of isotropic conductive adhesives," J. Electron. Mater. **38**, 430–437 (2009).
[11]H.-V. Nguyen, E. Andreassen, H. Kristiansen, and K. E. Aasmundtveit, "Die shear testing of a novel isotropic conductive adhesive–epoxy filled with metal-coated polymer spheres," IEEE Trans. Compon. Packag. Manuf. Technol. **3**, 1084–1093 (2013).
[12]S. Jain, "Isotropically conductive adhesive filled with silver metalised polymer spheres," Ph.D. thesis (Loughborough University, United Kingdom, 2016).
[13]H.-V. Nguyen, H. Kristiansen, J. Gakkestad, R. Johannessen, N. Høivik, and K. E. Aasmundtveit, "Spherical polymer particles in isotropic conductive adhesives a study on rheology and mechanical aspects," in *3rd Electronics System Integration Technology Conference ESTC* (IEEE, 2010), pp. 1–6.
[14]H.-V. Nguyen, H. Kristiansen, R. Johannessen, E. Andreassen, A. Larsson, and K. E. Aasmundtveit, "Temperature dependence of mechanical properties of isotropic conductive adhesive filled with metal coated polymer spheres," in *IEEE 61st Electronic Components and Technology Conference (ECTC)* (IEEE, 2011).
[15]H.-V. Nguyen, J. He, T. Helland, H. Kristiansen, and K. E. Aasmundtveit, "Electrical characterization of individual metal-coated polymer spheres used in isotropic conductive adhesives," J. Appl. Polym. Sci. **133**, 43764–43773 (2016).
[16]S. Jain, D. Whalley, M. Cottrill, H. Kristiansen, K. Redford, C. Nilsen, T. Helland, and C. Liu, "Electrical properties of an isotropic conductive adhesive filled with silver coated polymer spheres," in *18th European Microelectronics Packaging Conference* (IEEE, 2011), pp. 1–7.
[17]S. Jain, D. C. Whalley, M. Cottrill, T. Helland, H. Kristiansen, K. Redford, and C. Liu, "The effect of coating thickness on the electrical performance of novel isotropic conductive adhesives prepared using metallised polymer microspheres," in *2013 IEEE 63rd Electronic Components and Technology Conference* (IEEE, 2013), pp. 796–802.
[18]H.-V. Nguyen, K. E. Aasmundtveit, H. Kristiansen, and T. Helland, "An overview of isotropic conductive adhesives filled with metal-coated polymer spheres," International Symposium on Microelectronics **2013**, 000200–000207 (2013).

[19]J. Gakkestad, P. Dalsjø, H. Kristiansen, R. Johannessen, and M. M. V. Taklo, "Use of conductive adhesive for MEMS interconnection in ammunition fuze applications," J. Micro/Nanolithogr., MEMS, MOEMS **9**, 041108 (2010).
[20]J. Gakkestad, Z. Li, T. Helland, and C. P. Wong, "Thermo-mechanical properties of isotropic conductive adhesive filled with Metallized Polymer Spheres," in *2013 IEEE 15th Electronics Packaging Technology Conference (EPTC 2013)* (IEEE, 2013), pp. 213–218.
[21]H. Kristiansen, K. Redford, S. Helland, E. Kalland, N. H. Høglund, M. A. Ras, C. Grosse, B. Hay, L. Ramiandrisoa, G. Davée, S. Gomés, and S. R. Pettersen, "Thermal conduction in novel isotropic conductive adhesive," in *2017 23rd International Workshop on Thermal Investigations of ICs and Systems (THERMINIC)* (IEEE, 2017), pp. 1–5, iSSN: 2474-1523.
[22]S. R. Pettersen, S. Nagao, H. Kristiansen, S. Helland, J. Njagi, K. Suganuma, Z. Zhang, and J. He, "Investigation of thermal transport in polymer composites with percolating networks of silver thin films by the flash diffusivity method," J. Appl. Phys. **121**, 025101 (2017).
[23]D. G. Cahill, "Thermal conductivity measurement from 30 to 750 K: The 3ω method," Rev. Sci. Instrum. **61**, 802–808 (1990).
[24]D. G. Cahill, "Erratum: "Thermal conductivity measurement from 30 to 750 K: The 3ω method" [Rev. Sci. Instrum. 61, 802 (1990)]," Rev. Sci. Instrum. **73**, 3701 (2002).
[25]T. Borca-Tasciuc and G. Chen, "Experimental techniques for thin-film thermal conductivity characterization," in *Thermal Conductivity: Theory, Properties, and Applications*, Physics of Solids and Liquids, edited by T. M. Tritt (Springer US, Boston, MA, 2004), pp. 205–237.
[26]J. Moon, K. Weaver, B. Feng, H. Gi Chae, S. Kumar, J.-B. Baek, and G. P. Peterson, "Note: Thermal conductivity measurement of individual poly (ether ketone)/carbon nanotube fibers using a steady-state dc thermal bridge method," Rev. Sci. Instrum. **83**, 016103 (2012).
[27]F. Chen, J. Shulman, Y. Xue, C. W. Chu, and G. S. Nolas, "Thermal conductivity measurement under hydrostatic pressure using the 3ω method," Rev. Sci. Instrum. **75**, 4578–4584 (2004).
[28]D.-W. Oh, A. Jain, J. K. Eaton, K. E. Goodson, and J. S. Lee, "Thermal conductivity measurement and sedimentation detection of aluminum oxide nanofluids by using the 3ω method," Int. J. Heat Fluid Flow **29**, 1456–1461 (2008).
[29]M. L. Bauer and P. M. Norris, "General bidirectional thermal characterization via the 3ω technique," Rev. Sci. Instrum. **85**, 064903 (2014).
[30]R. M. Rodríguez-Laguna, A. Castro-Alvarez, M. Sledzinska, J. Maire, F. Costanzo, B. Ensing, M. Pruneda, P. Ordejón, C. M. S. Torres, P. Gómez-Romero, and E. Chávez-Ángel, "Mechanisms behind the enhancement of thermal properties of graphene nanofluids," Nanoscale **10**, 15402–15409 (2018).
[31]S. D. Lubner, J. Choi, G. Wehmeyer, B. Waag, V. Mishra, H. Natesan, J. C. Bischof, and C. Dames, "Reusable bi-directional 3ω sensor to measure thermal conductivity of 100-μm thick biological tissues," Rev. Sci. Instrum. **86**, 014905 (2015).
[32]C. Grosse, M. A. Ras, A. Varpula, K. Grigoras, D. May, M. Prunnila, and B. Wunderle, "Thermal characterization of thermal interface materials using the three-omega method," in *2018 7th Electronic System-Integration Technology Conference (ESTC)* (IEEE, 2018), pp. 1–4.
[33]C. Dames, "Measuring the thermal conductivity of thin films: 3 omega and related electrothermal methods," Annu. Rev. Heat Transfer **16**, 7 (2013).
[34]T. Borca-Tasciuc, A. R. Kumar, and G. Chen, "Data reduction in 3ω method for thin-film thermal conductivity determination," Rev. Sci. Instrum. **72**, 2139–2147 (2001).
[35]G. Avenue and W. Chester, "SPI supplies® brand quartz slides and cover slips."
[36]M. Bazilchuk, T. Sumigawa, T. Kitamura, Z. Zhang, H. Kristiansen, and J. He, "Contact area measurement of micron-sized metal-coated polymer particles under compression," Int. J. Mech. Sci. **165**, 105214 (2020).
[37]W. J. Kim, M. Taya, and M. N. Nguyen, "Electrical and thermal conductivities of a silver flake/thermosetting polymer matrix composite," Mechanics of Materials The Special Issue in Honor of Leon M. Keer **41**, 1116–1124 (2009).
[38]R. Franz and G. Wiedemann, "Ueber die Warme-Leitungsfahlkigheit der Metalle," Ann. Phys. **165**, 497–531 (1853).
[39]H. Kristiansen, S. Helland, E. Kalland, M. A. Ras, and C. Grosse, "Electrical and thermal conduction of isotropic conductive adhesive based on novel conductive particles," in *2018 IMAPS Nordic Conference on Microelectronics Packaging (NordPac)* (IEEE, 2018), pp. 40–44.
[40]S. R. Pettersen, H. Kristiansen, S. Nagao, S. Helland, J. Njagi, K. Suganuma, Z. Zhang, and J. He, "Contact resistance and metallurgical connections between silver coated polymer particles in isotropic conductive adhesives," J. Electron. Mater. **45**, 3734–3743 (2016).
[41]H.-K. Lyeo and D. G. Cahill, "Thermal conductance of interfaces between highly dissimilar materials," Phys. Rev. B **73**, 144301 (2006).
[42]S. I. Anisimov, B. L. Kapeliovich, and T. L. Perel'man, "Electron emission from metal surfaces exposed to ultrashort laser pulses," Sov. Phys. JETP **39**, 775 (1974).
[43]X. Yang, C. Liang, T. Ma, Y. Guo, J. Kong, J. Gu, M. Chen, and J. Zhu, "A review on thermally conductive polymeric composites: Classification, measurement, model and equations, mechanism and fabrication methods," Advanced Composites and Hybrid Materials **1**, 207–230 (2018).
[44]"Standard test method for thermal transmission properties of thermally conductive electrical insulation materials," Tech. Rep. (ASTM International, West Conshohocken, PA, 2017).
[45]ASTM E1461-13 "Standard test method for thermal diffusivity by the flash method," Tech. Rep. (ASTM International, West Conshohocken, PA, 2013).
[46]D. G. Cahill and R. O. Pohl, "Thermal conductivity of amorphous solids above the plateau," Phys. Rev. B **35**, 4067–4073 (1987).
[47]S. Sandell, E. Chávez-Ángel, A. El Sachat, J. He, C. M. Sotomayor Torres, and J. Maire, "Thermoreflectance techniques and Raman thermometry for thermal property characterization of nanostructures," J. Appl. Phys. **128**, 131101 (2020).